Suppl. Figure 1

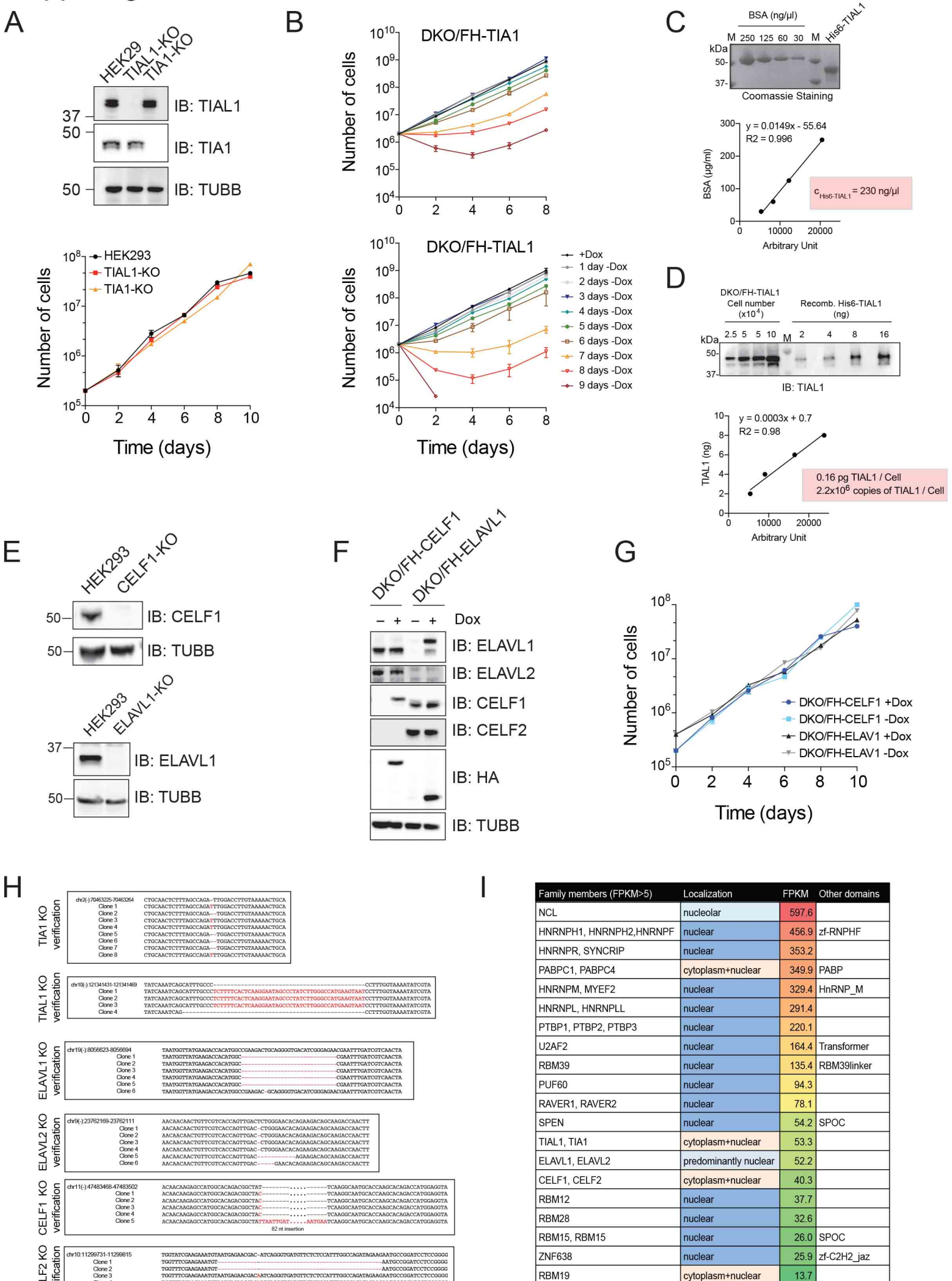

I

Family members (FPKM>5)	Localization	FPKM	Other domains
NCL	nucleolar	597.6	
HNRNPH1, HNRNPH2,HNRNPF	nuclear	456.9	zf-RNPHF
HNRNPR, SYNCRIP	nuclear	353.2	
PABPC1, PABPC4	cytoplasm+nuclear	349.9	PABP
HNRNPM, MYEF2	nuclear	329.4	HnRNP_M
HNRNPL, HNRNPLL	nuclear	291.4	
PTBP1, PTBP2, PTBP3	nuclear	220.1	
U2AF2	nuclear	164.4	Transformer
RBM39	nuclear	135.4	RBM39linker
PUF60	nuclear	94.3	
RAVER1, RAVER2	nuclear	78.1	
SPEN	nuclear	54.2	SPOC
TIAL1, TIA1	cytoplasm+nuclear	53.3	
ELAVL1, ELAVL2	predominantly nuclear	52.2	
CELF1, CELF2	cytoplasm+nuclear	40.3	
RBM12	nuclear	37.7	
RBM28	nuclear	32.6	
RBM15, RBM15	nuclear	26.0	SPOC
ZNF638	nuclear	25.9	zf-C2H2_jaz
RBM19	cytoplasm+nuclear	13.7	
RBM45	cytoplasm	11.3	

Figure S1: Double knockout of TIA1 and TIAL1 causes cell death (related to Figure 1).

A) Upper panel: IB analysis to verify CRISPR-Cas9-mediated TIA1 or TIAL1 single gene knockouts in HEK293 cells using protein-specific antibodies, respectively. Lysate of parental HEK293 cells was used for comparison. Detection of β-tubulin (TUBB) served as loading control. Lower panel: Proliferation of parental HEK293 cells and TIA1 (TIA1-KO) or TIAL1 (TIAL1-KO) single knockout HEK293 cells over a time period of 10 days. **B)** DKO/FH-TIA1 (left) and DKO/FH-TIAL1 (right) cells were cultured in Dox-free media for up to 9 days before recording cellular proliferation. At day 0, 2,000,000 cells were seeded and cultured in Dox-supplemented media. Cells were counted over a period of 8 days. **C)** Recombinant His6-tagged TIAL1 was separated via SDS-PAGE along with increasing amounts of BSA to estimate the concentration of purified TIAL1 protein. Signal intensities of Coomassie stained protein bands were quantified using ImageJ software and plotted against the amount of BSA. The regression line, coefficient of determination (R2) and the calculated concentration of His6-TIAL1 are given. **D)** 2.5-10×104 DKO/FH-TIAL1 cells per lane of a SDS-PAGE gel and increasing amounts of purified His6-tagged TIAL1 (2-16 ng) were separated via SDS-PAGE, blotted and probed with an anti-TIAL1 antibody. Protein bands were detected by chemiluminescence, intensities quantified using ImageJ software and plotted against the amount of TIAL1 protein. The regression line, coefficient of determination (R2) and the calculated amount of FH-tagged TIAL1 per cells are given. **E)** IB analysis to verify CRISPR-Cas9-mediated ELAVL1 or CELF1 single gene knockouts using antibodies specific for human ELAVL1 or CELF1, respectively. Lysates of parental HEK293 cells were loaded for comparison. Detection of β-tubulin (TUBB) served as loading control. **F)** IB analyses to verify the CRISPR-Cas9-mediated ELAVL1 and ELAVL2 as well as CELF1 and CELF2 double gene knockout in HEK293 cells inducibly expressing FH-tagged ELAVL1 or FH-tagged CELF1. Depletion of Dox for 10 days strongly decreased levels of FH-tagged proteins. Detection of β-tubulin (TUBB) served as loading control. **G)** Proliferation of ELAVL1/ELAVL2 or CELF1/CELF2 double knockout HEK293 cells inducibly expressing FH-tagged ELAVL1 or CELF1, respectively, cultured in the presence (+Dox) or absence (-Dox) of Dox. **H)** Verification of the CRISPR-Cas9-mediated gene knockouts of TIA1, TIAL1, ELAVL1, ELAVL2, CELF1, and CELF2 by PCR amplification and cloning of the genomic locations of the CRISPR editing event into pCR-blunt. 4-10 clones were sequenced. **I)** The TIA1 family of proteins is one of more than 20 U-rich RBPs families comprising 3 or more RRMs and show expression in HEK293 cells (FPKM ≥ 5). Additionally, the predominant subcellular localization, the sum of the expression values of individual family members (FPKM), and protein domains other than the 3 RRMs are given.

Suppl. Figure 2

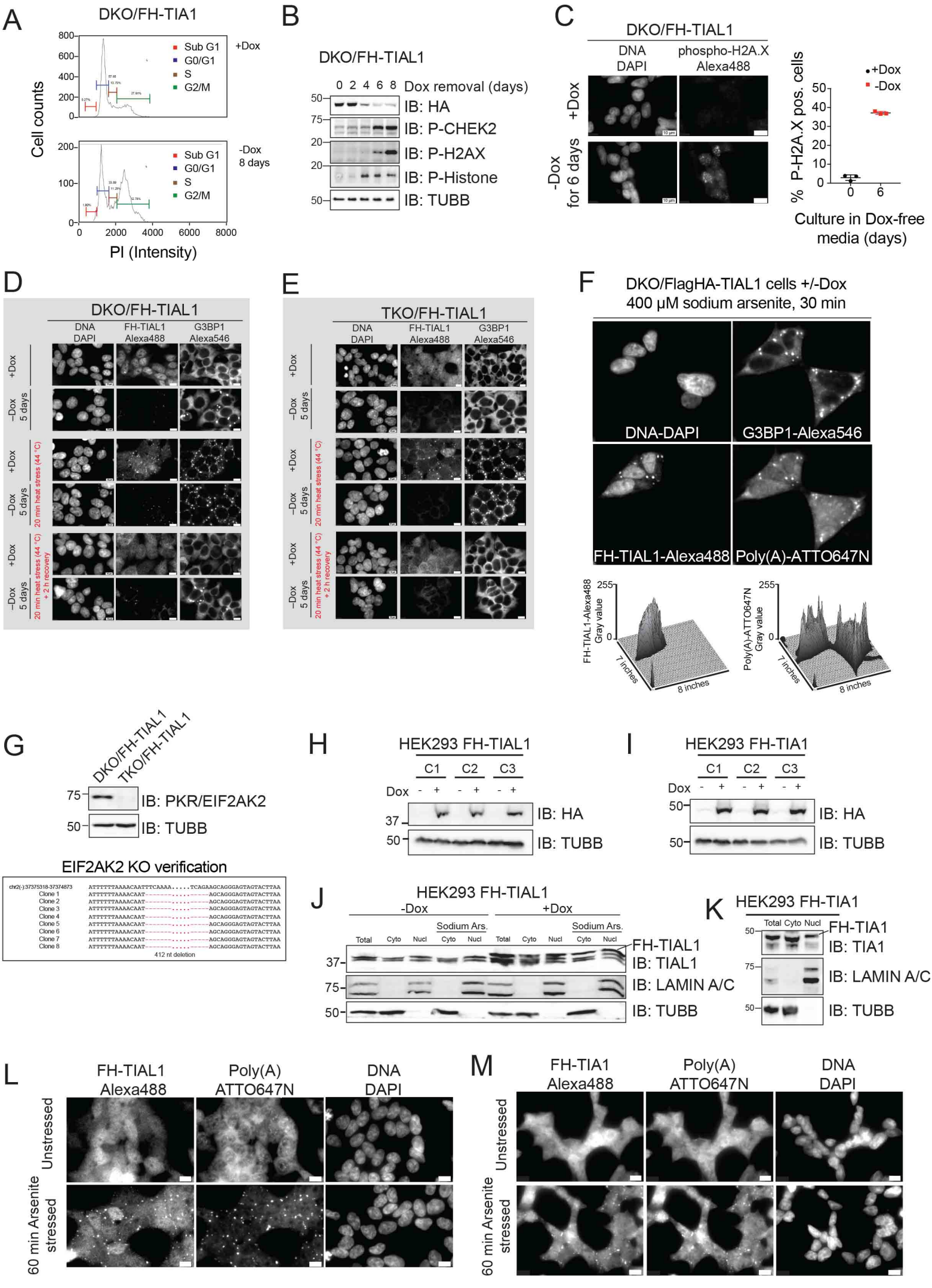

Figure S2: Double knockout of TIA1 and TIAL1 causes stress granule formation (related to Figures 2 and 3). A) Example raw profiles of cell cycle analyses performed on DKO/FH-TIA1 cells cultured with or without Dox for 8 days (see also Figure 1D). **B)** DKO/FH-TIAL1 cells cultured in Dox-free media for up to 8 days show signs of damaged DNA and activated DNA damage response indicated by increased phosphorylation of Serine/threonine-protein kinase CHEK2 and Histone H2AX as verified by IB using phospho-CHEK2 and phospho-H2AX-specific antibodies, respectively. Additionally, IB analyses revealed increase in phosphorylation of Histone H3 at Ser10. **C)** DKO/FH-TIAL1 cells cultured with or without Dox for 6 days were fixed and phosphorylation of H2AX visualized by IF staining. Cells positive for phosphorylated H2AX were counted based on fluorescence micrographs. 35% of DKO/FH-TIAL1 cells cultured in Dox-free media for 6 days showed phosphorylation of H2AX. Nuclei were stained with DAPI. Scale bar, 10 µm. **D,E)** DKO/FH-TIAL1 **(D)** or TKO/FH-TIAL1 **(E)** cells show no defects in SG assembly or disassembly if exposed to heat shock as analyzed by multicolor IF. Cells were cultured with or without Dox for 5 days. Cells were either left untreated (upper panels), or exposed to heat shock at 44 °C for 20 min (middle panels), or exposed to heat shock at 44 °C for 20 min followed by a 2-hr recovery period at 37 °C (lower panels). After fixation, cells were immunostained for FH-tagged TIAL1 and G3BP1, respectively. Localization of proteins was visualized by fluorescence microscopy. Nuclei were stained with DAPI. Scale bar, 10 µm. **F)** Upper panels: Subcellular localization of TIAL1, G3BP1 and poly(A)-mRNAs in DKO/FH-TIAL1 cells cultured with or without Dox for 6 days detected by RNA-FISH and IF. DAPI was used for staining of nuclear DNA. Lower panels depict maps (Image J) of TIAL1 and poly(A)-mRNA fluorescence signals according two the images above. **G)** Upper panel: Verification of the CRISPR-Cas9-mediated EIF2AK2 gene knockout in DKO/FH-TIAL1 cells by IB analysis. Lower panel: cloning of the genomic locations of the CRISPR editing event to verify the CRISPR-Cas9-mediated EIF2AK2 gene knockout in DKO/FH-TIAL1 cells. **H,I)** Generation of stable HEK293 cells expressing FH-tagged TIAL1 **(H)** or TIA1 **(I)** under control of Dox-inducible promoter. Clone 1 was selected for further experiments. **J,K)** TIAL1 (with or without stress treatment) **(J)** or TIA1 **(K)** proteins show equal nuclear and cytoplasmic distribution as revealed by nucleo-cytoplasmic fractionation of HEK293 cells inducibly expressing FH-tagged TIAL1 or FH-tagged TIA1, respectively. IB analysis was performed on total cell lysate (Total), the cytoplasmic fraction (Cyto), as well as the nuclear fraction (Nucl). TIAL1 and TIA1 were detected using protein-specific antibodies. Detection of LaminA/C for nuclear fraction, TUBB for cytoplasmic fraction. **L,M)** Subcellular localization of FH-tagged TIAL1 **(L)** or FH-tagged TIA1 **(M)** in HEK293 cells with or without exposing the cells to sodium arsenite (60 min, 400 µM) was determined by IF. Detection of poly(A)-mRNAs by RNA-FISH. Nuclei were stained with DAPI. All FH-tagged proteins co-localized with poly(A)-mRNAs to SG upon oxidative stress treatment.

Suppl. Figure 3

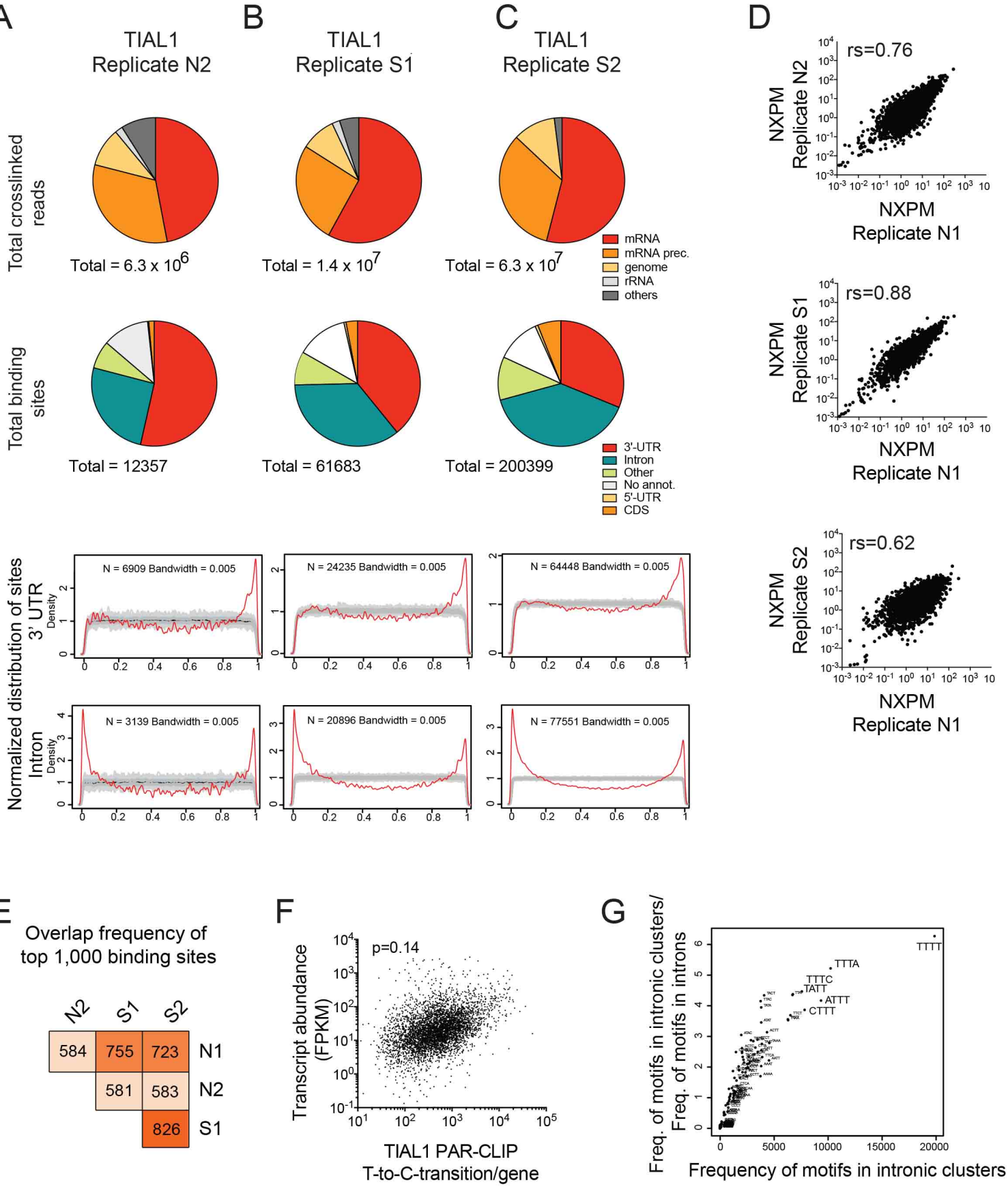

Figure S3: TIAL1 PAR-CLIP performed in HEK293 cells without or with exposure to oxidative stress (related to Figure 3). A-C) PAR-CLIP data analyses for TIAL1 performed on FH-tagged TIAL1 expressing HEK293 cells under normal growth conditions (**A**, Normal growth Replicate N2) or when cells were exposed to sodium arsenite stress for 60 min (**B**, Replicate S1; **C**, Replicate S2). From top to bottom: i) Total crosslinked T-to-C reads originating from the corresponding TIAL1 PAR-CLIP mapping to different RNA categories using the PAR-CLIP suite pipeline (Garzia et al., 2017). The total number of crosslinked reads is given for each replicate. ii) PARalyzer-based distribution of TIAL1 binding sites across mRNAs. The total number of binding sites is given for each replicate. iii) Normalized density of TIAL1 PAR-CLIP binding sites over 3' UTRs (red lines) compared to a randomized background (grey lines) as determined by PARalyzer. iv) Normalized density of TIAL1 PAR-CLIP binding sites over intronic regions (red lines) compared to a randomized background (grey lines) as determined by PARalyzer. **D)** Scatterplots of NXPM (normalized crosslinked reads per million) values of each target mRNA in all four TIAL1 PAR-CLIP data sets (N1, N2, S1, and S2, respectively) performed in FH-TIAL1 expressing HEK293 cells under normal (N) or sodium arsenite stressed (S) growth conditions. The spearman correlation is indicated. **E)** Overlap frequencies of the top 1,000 crosslinked clusters of each TIAL1 PAR-CLIP replicate (N1, N2, S1, and S2, respectively) based on the total number of sequence reads per cluster (T-to-C fraction ≥ 0.3). **F)** Scatterplot depicting the correlation between T-to-C transitions per gene for the TIAL1 PAR-CLIP replicate N1 and mRNA abundance (FPKM) in parental HEK293 cells derived from poly(A)-RNA-seq. Spearman correlation is indicated. **G)** kmer-plot of the TIAL1 RRE derived from PAR-CLIP binding sites in intronic regions of target mRNAs.

Suppl. Figure 4

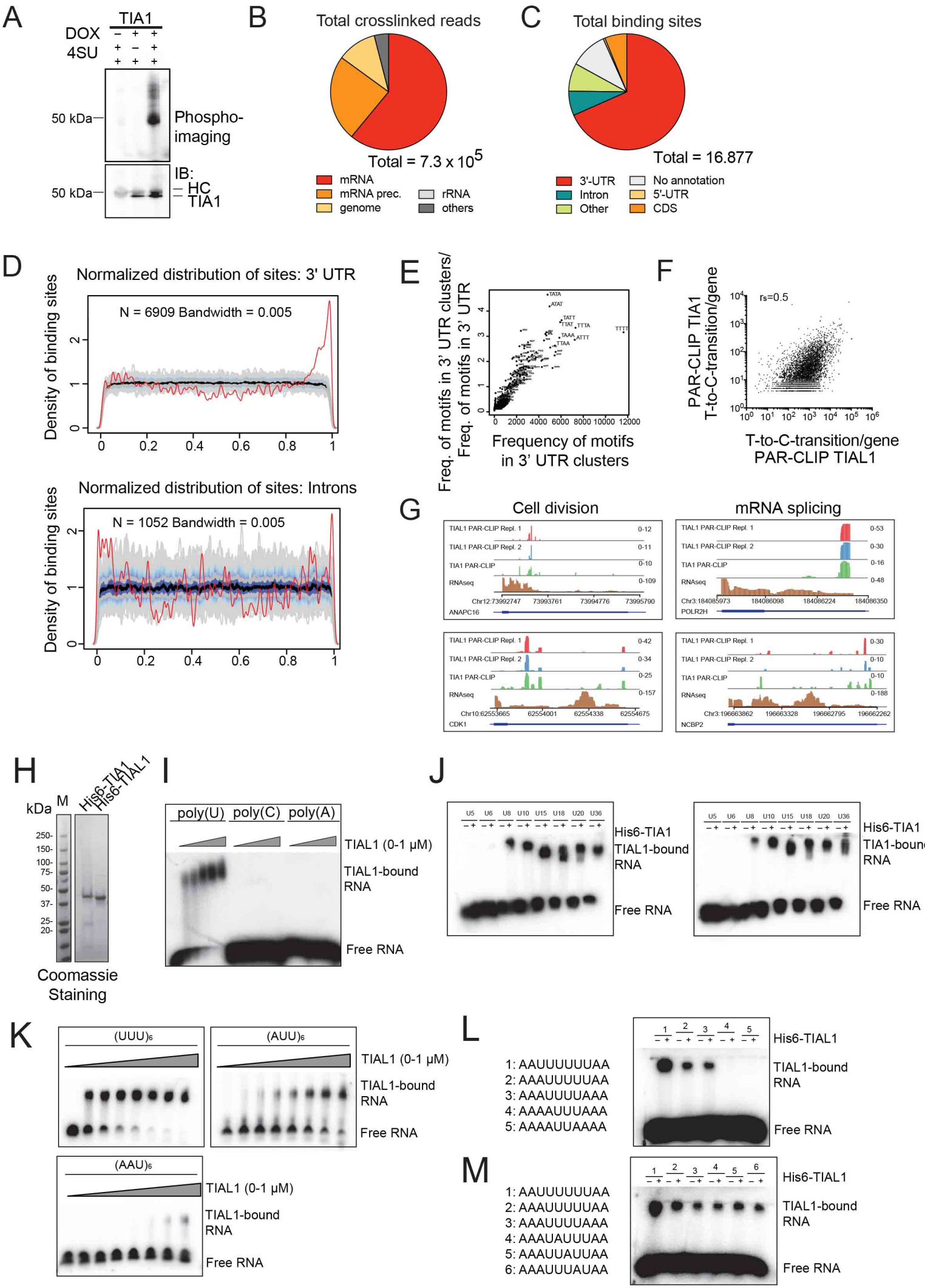

Figure S4: TIA1 proteins bind U-rich RNAs (related to Figure 3). A) Upper panels: Autoradiograph of crosslinked and 5'-end radiolabeled RNA- TIA1 complexes immunoprecipitated from FH-TIA1 expressing HEK293 cells and separated by SDS-PAGE following 4SU PAR-CLIP. Lower panel: IB analysis of the crosslinked immunoprecipitate using an anti-HA antibody. HC, Heavy chain; XL, crosslinking. **B)** Total crosslinked T-to-C reads originating from the TIA1 PAR-CLIP mapping to different RNA categories using the PAR-CLIP suite pipeline (Garzia et al., 2017). The total number of crosslinked reads is given. **C)** PARalyzer-based distribution of TIA1-crosslinked sequence reads resulting from PAR-CLIP performed under normal growth conditions. **D)** Normalized density of TIA1 PAR-CLIP binding sites over the 3' UTR (left panel, red lines) or over the introns (right panel, red lines) compared to a randomized background (grey lines) as determined by PARalyzer (Corcoran et al., 2011). **E)** kmer-plot of the TIA1 RRE derived from PAR-CLIP binding sites in 3' UTRs of target mRNAs. **F)** Scatterplot of the average T-to-C transitions per gene for the TIAL1 PAR-CLIP replicate N1 versus the TIA1 PAR-CLIP. Pearson correlation is indicated. **G)** Sequence read coverage plots illustrating the 3'-end portions of representative targets mRNAs involved in 'Cell division' or 'mRNA splicing'. Coverage tracks include HEK293 poly(A)-mRNA-seq data along with mapped sequence reads of FH–TIAL1 as well as FH-TIA1 PAR-CLIPs. **H)** N-terminally 6x-His-tagged TIA1 and TIAL1 were expressed in *E. coli* BL21 DE3 cells and purified by IMAC. SDS-PAGE fractionated and Coomassie-stained fractions of purified proteins are shown. M, protein marker. **I)** Purified TIAL1 protein (0–1 µM) was incubated with radiolabeled 18-nt poly(U), poly(C), and poly(A) and RNA-protein complexes were separated from unbound RNA by 1.5% agarose gel electrophoresis. Protein binding was only observed for poly(U). **J)** Definition of the minimal number of nucleotides required for TIA1 and TIAL1 binding to target RNA. TIAL1 (left panel) or TIA1 protein (right panel) were incubated with radiolabeled poly(U) of different length (5-36 nt) and separated on a 1.5% agarose gel. Synthetic RNAs of 8 nucleotides or longer were sufficient for protein binding. **K)** TIAL1 protein (0 – 1 µM) was incubated with radiolabeled trinucleotide repeats (UUU)6, (AUU)6, or (AUU)6 separated on a 1.5% agarose gel, respectively. **L)** Purified TIAL1 (1 µM) was incubated with radiolabeled (U)10 as well as different 10mers reducing the length of the U-stretch by increasing the number of flanking As. **M)** EMSA of purified TIAL1 (1 µM) and radiolabeled 10mers disturbing the minimal U4 by insertion of As at different positions.

Suppl. Figure 5

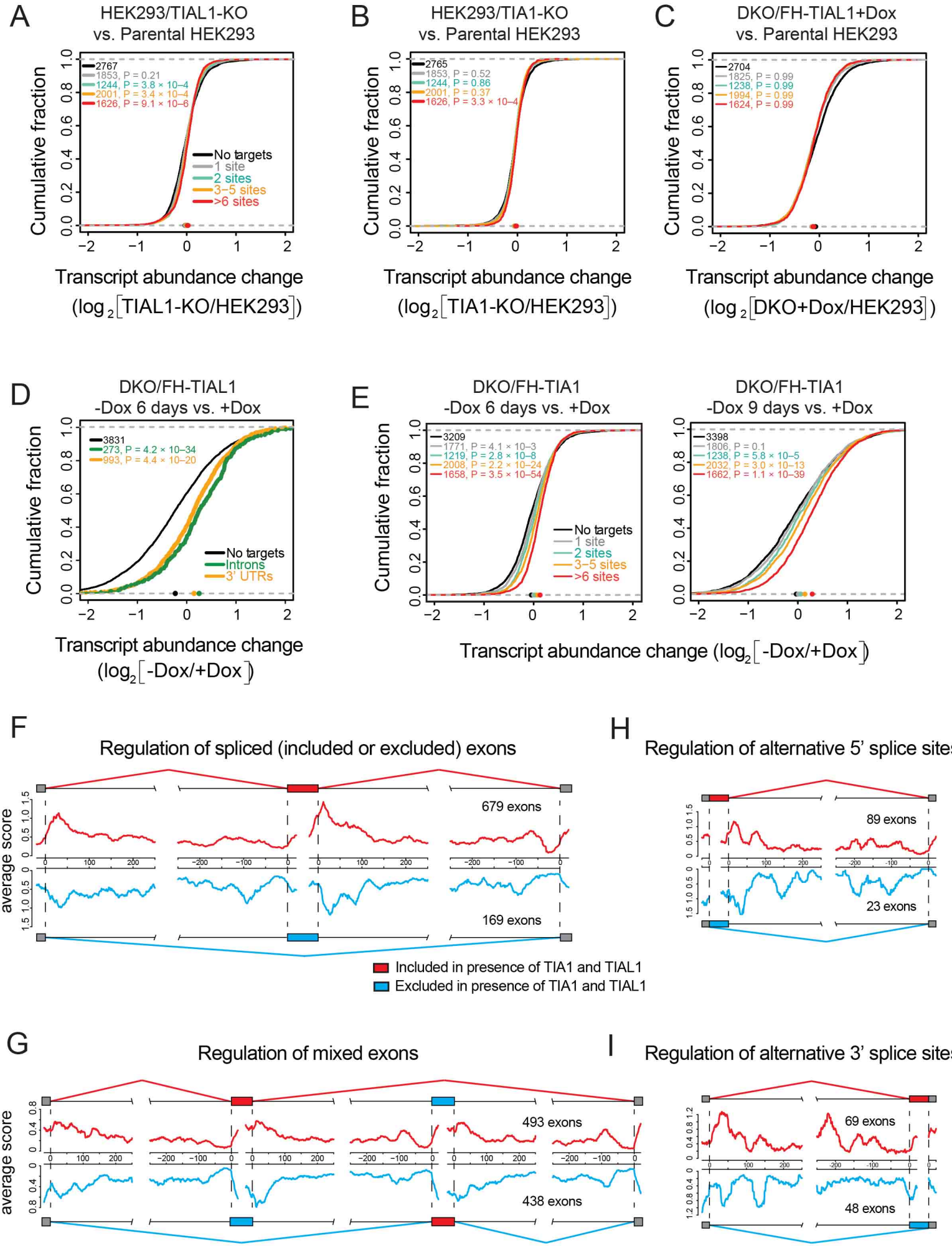

Figure S5: TIA1 proteins regulate mRNA stability and alternative splicing (related to Figure 4). A-C) The empirical cumulative distribution function (CDF) to analyze mRNA expression changes in TIAL1 single KO cells **(A)**, TIA1 single KO cells **(B)** or DKO/FH-TIAL1 cells grown with Dox **(C)** in comparison to parental HEK293 cells as determined by poly(A)-RNA-seq. TIAL1 PAR-CLIP targets were binned by number of binding sites and compared to expressed non-targets (FPKM ≥3, black line). Dots on the x-axis indicate the median change. The Mann–Whitney U test was used to determine P values. **D)** The CDF illustrating mRNA expression changes in DKO/FH-TIAL1 cells cultured with (+Dox) or without Dox (-Dox) for 6 days as determined by poly(A)-RNA-seq. TIAL1 PAR-CLIP targets were binned by targets with ≥3 intronic binding sites (and no binding sites in 3' UTRs) or with ≥3 binding sites in 3' UTRs (and no binding sites in introns) compared to expressed non-targets (FPKM ≥3, black line). Dots on the x-axis indicate the median change. The Mann–Whitney U test was used to determine P values. **E)** mRNA expression changes in DKO/FH-TIA1 cells cultured with (+Dox) or without Dox (-Dox) for 6 or 9 days as determined by poly(A)-RNA-seq. Shown is the CDF of TIAL1 PAR-CLIP targets binned by number of binding sites compared to expressed non-targets (FPKM ≥3, black line). Dots on the x-axis indicate the median change. The Mann–Whitney U test was used to determine P values. **F-I)** TIAL1 RNA splicing maps reveal consistent binding patterns for both included and excluded spliced exons **(F)**, mixed exons **(G)**, exons with alternative 5' SS **(H)**, or exons with alternative 3' SS **(I)**. For a full list of AS events see Table S4.

Suppl. Figure 6

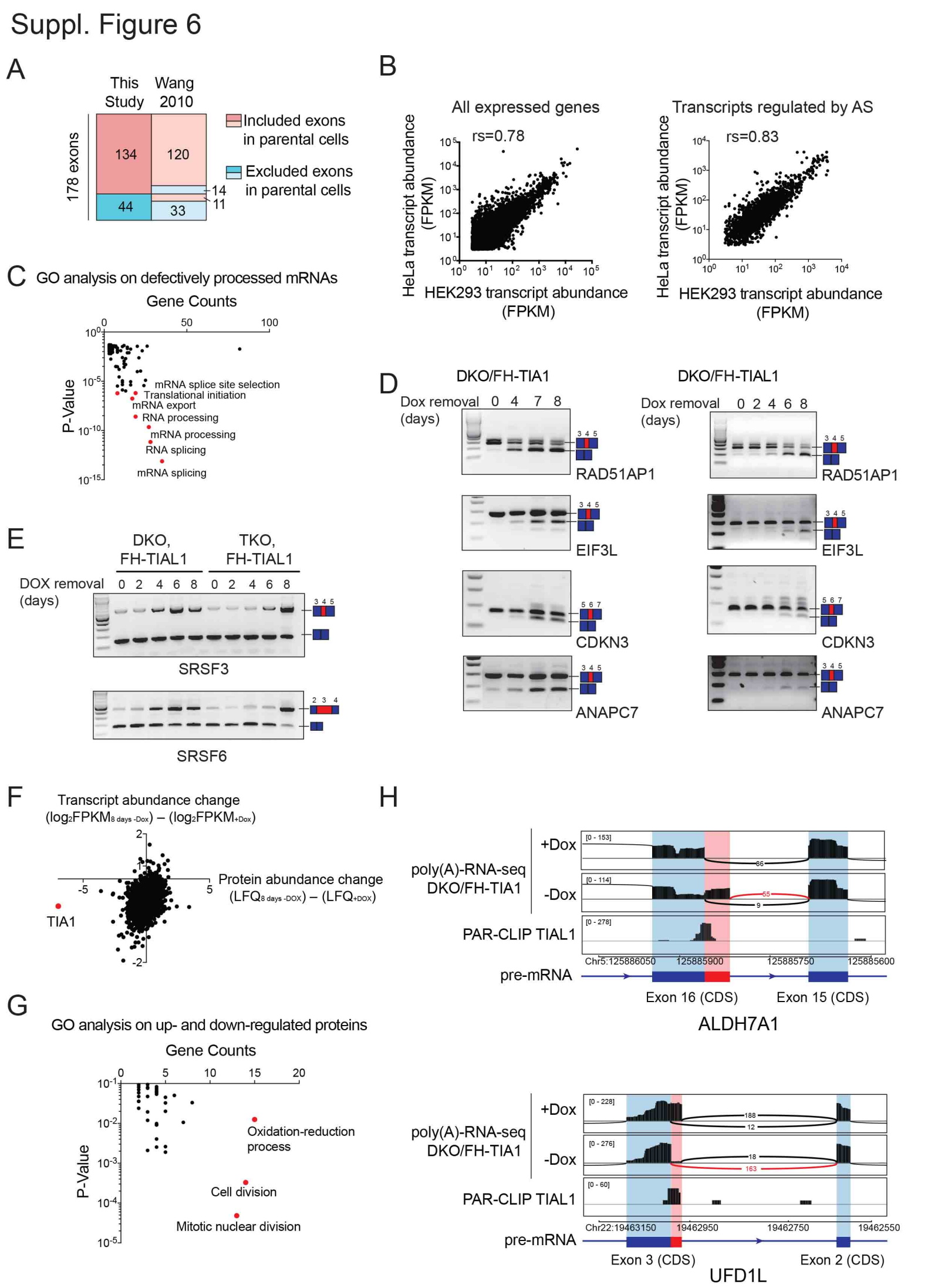

Figure S6: Loss of TIA1 proteins causes defects in alternative splicing (related to Figure 5). A) Overlap of significant AS events occurring upon CRISPR-Cas9-mediated TIA1/TIAL1 DKO in HEK293 cells (this study, FDR < 0.05) and siRNA-mediated knockdown of TIA1 and TIAL1 in HeLa cells (|∆Irank|>1) (Z. Wang et al., 2010). **B)** Scatterplots depicting the correlation between transcript abundance (FPKM) of all mRNAs (left) or mRNAs regulated by AS (right) in either HEK293 or HeLa cells. Spearman correlation is indicated. **C)** GO analysis of mRNAs significantly differentially spliced in DKO/FH-TIA1 or DKO/FH-TIAL1 cells upon removal of Dox. Top GO terms ranked by p-value are shown. For a complete list see Table S4. **D)** RT-PCR to verify significant AS events occurring upon depletion of Dox (0, 4, 7, 8 days) in DKO/FH-TIA1 (left panels) or upon depletion of Dox (0, 2, 4, 6, 8 days) in DKO/FH-TIAL1 cells (right panels). Boxes in red represent alternatively spliced exons. Selected genes are representative members of the GO enrichment terms "cell division" (RAD51AP1, ANAPC7, CDKN3), and "translation initiation" (EIF3L). **E)** RT-PCR to verify significant AS events occurring upon depletion of Dox (0, 2, 4, 6, 8 days) in DKO and TKO/FH-TIAL1 cells. **F)** Scatterplot depicting the change in transcript abundance in DKO/FH-TIA1 cells grown with or without Dox for 8 days versus changes in protein abundance in DKO/FH-TIA1 cells cultured with or without Dox for 8 days. **G)** GO analysis of the 134 downregulated proteins when DKO/FH-TIA1 cells were grown in DOX-free media for 8 days. Top GO terms ranked by p-value are shown. For a complete list see Table S5. **H)** Histograms representing the poly(A)-RNA-seq coverage of DKO/FH-TIA1 cells cultured for 0 (+Dox) or 8 days in absence of Dox (-Dox) together with the depth of TIAL1 PAR-CLIP read coverage along the alternatively spliced exons and the flanking exons of the ALDH7A1 or UFD1L mRNAs. The arcs represent splice junctions with the number of reads mapped to the junction . The red box indicates the alternatively spliced exon. The blue boxes indicate constitutive exons.

Suppl. Figure 7

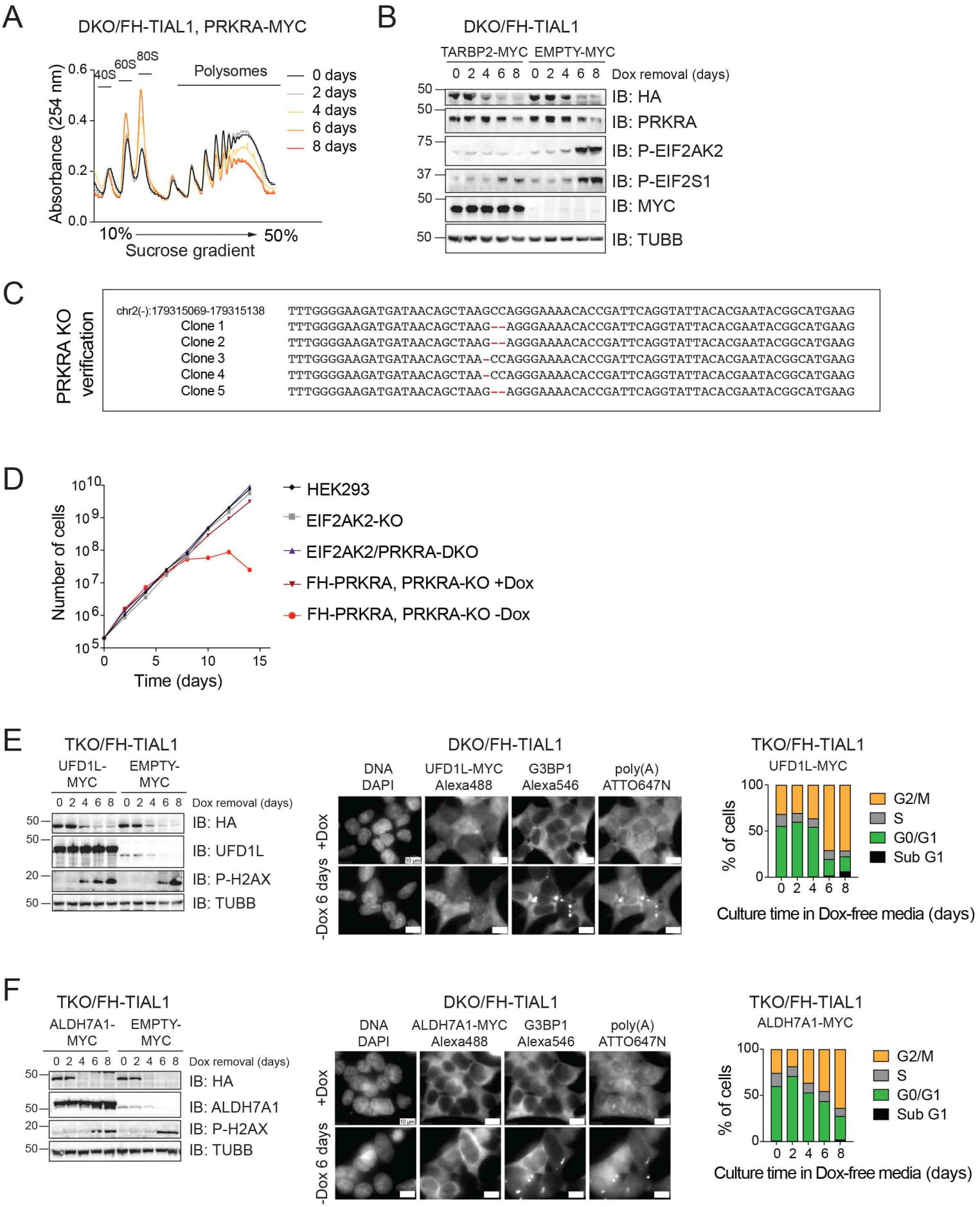

Figure S7: Loss of PRKRA in HEK293 cells causes cell death (related to Figure 6). A) Polysome profiling analysis of DKO/FH-TIAL1 cells expressing c-Myc-tagged PRKRA (PRKRA-MYC) cultured without Dox (0, 2, 4, 6, 8 days). **B)** Lysates of DKO/FH-TIAL1 cells either expressing c-Myc-tagged TARBP2 (TARBP2-MYC) or c-Myc alone (EMPTY-MYC) were analyzed for phosphorylated EIF2AK2 and phosphorylated EIF2S1 by IB analyses. Detection of TUBB served as loading control. **C)** Verification of the CRISPR-Cas9-mediated PRKRA gene KO in HEK293 cells expressing FH-tagged PRKRA carrying a silent point mutation in the PAM sequence to prevent targeting by Cas9. **D)** Proliferation of parental HEK293 cells, single EIF2AK2 KO cells, EIF2AK2/PRKRA DKO cells, as well as PRKRA-KO FH-PRKRA cells cultured in presence (+Dox) or absence (-Dox) of Dox over a 14-day time course. **E,F)** Lentiviral overexpression of c-Myc-tagged UFD1L **(E)** or ALDH7A1 **(F)** does not prevent SG formation or cell cycle arrest upon loss of TIA1 and TIAL1 function as revealed by IB analysis of TKO/FH-TIAL1 cells to detect phosphorylated H2AX (left panel), RNA-FISH combined with IF on DKO/FH-TIAL1 cells to detect SG formation (middle panel), or cell cycle analyses of TKO/FH-TIAL1 cultured with or without Dox for up to 8 days (right panel), respectively.